JOURNAL OF MATERIALS SCIENCE 27 (1992) 313-318

# Conductive $SnO_2$/Sb powder: preparation and optical properties

Z.CRNJAK OREL, B. OREL, M. HODOŠČEK, V. KAUČIČ
*Boris Kidrič Institute of Chemistry, 61 115 Ljubljana, POB 30, Yugoslavia*

Preparation of an $SnO_2$ semiconducting powder doped with antimony ($x = 2.38$ mol%) was achieved by co-precipitation. The unit cell parameters of the doped $SnO_2$ powders were measured and their changes with dopant concentration were determined. Four-point sheet resistance measurements, together with optical and infrared spectra of the powder were taken in order to obtain a highly-conducting, low-emitting powder which could be used for antistatic paint preparation. Evolution of the phonon bands corresponding to Sn–O stretching modes as a function of dopant concentration were followed, and a model calculation based on an extended four-parametric Kurosawa relation was applied to the reflection spectra of differently doped powders. It was found that the frequency of the plasma oscillations shifts with dopant concentration, and the intensity of the reflectivity peaks was correlated with plasmon–phonon interactions. An additional negative reflection peak in the range 1100 to 1200 $cm^{-1}$ was found in the reflection spectra of highly doped powders and was attributed to the coupled modes between the plasma oscillations and one of the phonon combinational or overtone modes of $SnO_2$.

## 1. Introduction

$SnO_2$ has been extensively investigated in the past because of the semiconducting properties which it exhibits in monocrystalline, powder or thin-layer forms [1]. Due to a wide band gap (3.8 eV), the absorption edge appears in the ultraviolet range (0.36 μm) which makes this compound transparent to visible and near infrared radiation. The free carrier concentration could be varied at will when thin layers of $SnO_2$ are formed, simply by changing the concentration of dopant atoms. The onset of free carrier absorption and/or reflection appears in the mid infrared and is described by the plasma frequency ($\omega_p$). $SnO_2$ acts as a spectrally selective window in which transparency and reflectivity can be controlled in order to meet requirements which are specific for particular applications [2–4]. Moreover, due to the high free carrier concentration of $10^{-20}$ $cm^{-3}$, $SnO_2$ also exhibits d.c. electrical conductivity which still further extends its applicability [5].

$SnO_2$ in thin film form is generally accepted as a transparent electrode and is used in photovoltaic devices and in "smart" window design, where electrochromism is exploited for controlling the solar radiation which enters the building through the glazing, thus decreasing the heat loads during the day, in particularly for hot climates [2].

Spectrally selective $SnO_2$ coatings on vitreous black enamel substrates [3] have been prepared for photothermal conversion of solar energy. In this configuration high infrared reflectivity, i.e. low emittance, depresses the thermal radiation losses from the warm-up solar collector panel surface. Although good spectral selectivity has been achieved (solar absorptance 0.9 and thermal emittance 0.13) [4], the preparation of large coatings on an industrial scale is difficult and requires sophisticated equipment. Achieving very high selectivity is impossible due to the high refractive index ($n$) of the coating and the consequent reflection of visible light. Nevertheless, the adherence, stability and durability of such a reflector/absorber tandem is satisfactory.

Similarly, $SnO_2$ deposited on glass has been used as a low-emittance coating in order to decrease radiative heat losses through window glazing [2]. Nevertheless, sprayed pyrolytically prepared coatings are not free of defects and their preparation is expensive.

It is generally accepted [2] that paint coatings could represent a much cheaper alternative for spectrally selective solar collector surfaces, and also as low-emittance coatings in window glazing. Besides a resin binder, such a paint should contain a conductive pigment and would also exhibit antistatic properties. So far [5,6], antistatic coatings have been confined mainly to carbon blacks and metallic pigments. Moreover, organic polymer binders were mostly cationic electrolytes and therefore sensitive to humidity and not suitable for exposure to external conditions.

An additional application of $SnO_2$ powders is their ability to prevent photolysis of $TiO_2$ pigments when they are formed by co-precipitation with $TiO_2$ [6]. Chaulking of paints, especially epoxies, would be minimized with application of such mixed pigments.

The structural properties of various Sn/Sb oxides have been studied by X-ray diffraction techniques, and the cell parameters correlated with d.c. electrical measurements [7, 8]. It was found, for example [9], that calcination temperatures above 1000 °C are needed to obtain proper dopant compounds. Too low calcination temperatures or too high an antimony

0022–2461/92 $03.00 + .12 

oxide content results in a phase-separated $Sb_2O_4$–$SnO_2$ system [9]. Optical spectra of $SnO_2$/Sb powders have been measured in order to determine the influence of crystallite size on the colour matching parameters [6].

The infrared spectra of conductive powders are difficult to measure. The $SnO_2$/Sb particle size should be in the range 0.3 to 0.4 μm in order to minimize the Mie type of scattering. This condition could be easily fulfilled for the infrared spectral region due to the longer wavelength of the infrared radiation. However, antimony-doped compounds exhibit a higher refractive index in the infrared due to the onset of plasma oscillations which makes it difficult to detect phonon bands in the transmission spectra.

In this paper, we report our attempts to prepare $SnO_2$ powder doped with antimony. The purpose of our work was not only to correlate the structural and optical properties of the powders, but to find the optimal concentration of antimony dopant atoms in order to obtain a semiconducting powder with the lowest possible thermal emittance.

## 2. Experimental procedure

The $SnO_2$/Sb powder was prepared by a co-precipitation method [10] from $SnCl_4 \cdot 5H_2O$ and $SbCl_3$ (Merck). The main purpose was to determine to what extent the concentration of antimony dopant atoms could be varied in the parent crystal. We started with a water solution of $SnCl_4 \cdot 5H_2O$ in which the $Sn^{4+}$ ion concentration was kept constant and to which $SbCl_3$ was added. In order to increase the solubility of $SbCl_3$, concentrated HCl was added. In a warm-up solution (95 °C) a pH of 3.2 was achieved. The resulting mixed hydroxide precipitate was washed alternately with $NH_4NO_3$ solution (to prevent peptization) followed by water until no trace of chloride ions could be detected. The precipitate was then peptized to release any further occluded chloride and uncoagulated with $NH_4NO_3$ solution. The final precipitate was in a colloidal state, its yellowish colour depending upon the concentration of antimony dopant. The precipitates were dried at 45 °C for 48 h and were afterwards calcined for 7 h at 1200 °C.

Fourier transform–infrared (FT–IR) spectra were recorded on a Digilab FTS-80 spectrophotometer equipped with a diffuse reflectance infrared cell (Drift-Barnes) with a collection solid angle of 30°. The samples were pressed into pellets, surfaces slightly polished and reflection spectra measured. Transmission spectra were recorded as nujol mulls or in KBr pellets.

Surface resistivity measurements were performed on an ordinary four-point measurement device (Faculty for Electrotechnology, Ljubljana). Unit cell parameters were determined using an X-ray diffraction unit (Philips).

## 3. Results and discussion

### 3.1. X-ray studies

X-ray diffraction studies [9] were carried out on powdered samples in which the concentration of dopant atoms had been previously determined by atomic absorption spectroscopy. The powders were finely ground and put into the sample carrier which were exposed to $K\alpha$ radiation in a Philips powder diffraction goniometer. In all cases a cassiterite pattern was produced. This was well developed for all the samples, containing various concentrations of antimony atoms (0–2.38 mol %). No spurious bands were detected which might have indicated the presence of the glassy state. A typical X-ray powder spectrum is presented in Fig. 1, and the results of the X-ray analysis are presented in Fig. 2.

Owing to the scattering of the results shown in Fig. 2, it was impossible to draw definite conclusions about the nature of the distortion of the cassiterite structure due to the presence of the impurity. The linear dependence of the unit cell parameters in the concentration range $0.05 < x < 0.023$ observed by Kikuchi and Umehara [9] was not detected due to the lack of samples having such small concentrations of dopant atoms. Unit cell dimension changes are of the same order as reported [9] but they are greater for the *a*- and not for the *c*-axis and do not increase linearly with dopant concentration. Independence of unit cell parameters at small dopant concentrations [9] was not observed due to an insufficient number of data points in this concentration range of dopant.

### 3.2. Visible and infrared spectra

The parameters of interest in low-emittance coatings and transparent coatings for solar radiation control

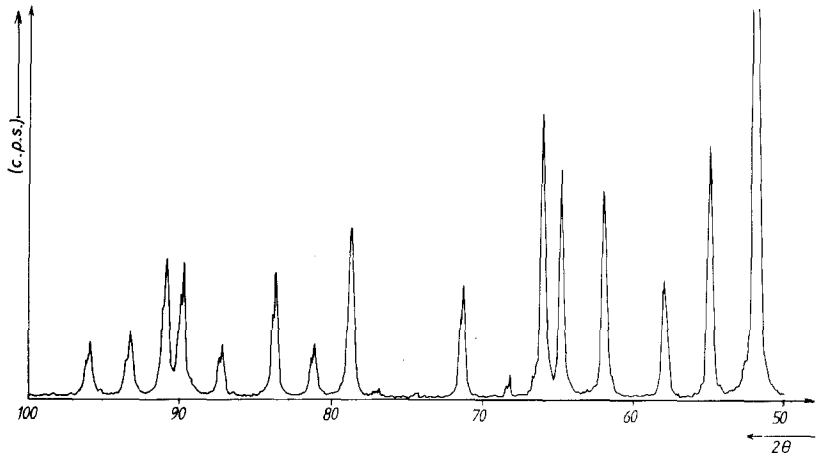


*Figure 1* Typical X-ray powder spectrum of doped $SnO_2$/Sb powder ($x = 0.5$ mol %, $50° < 2\theta < 100°$).

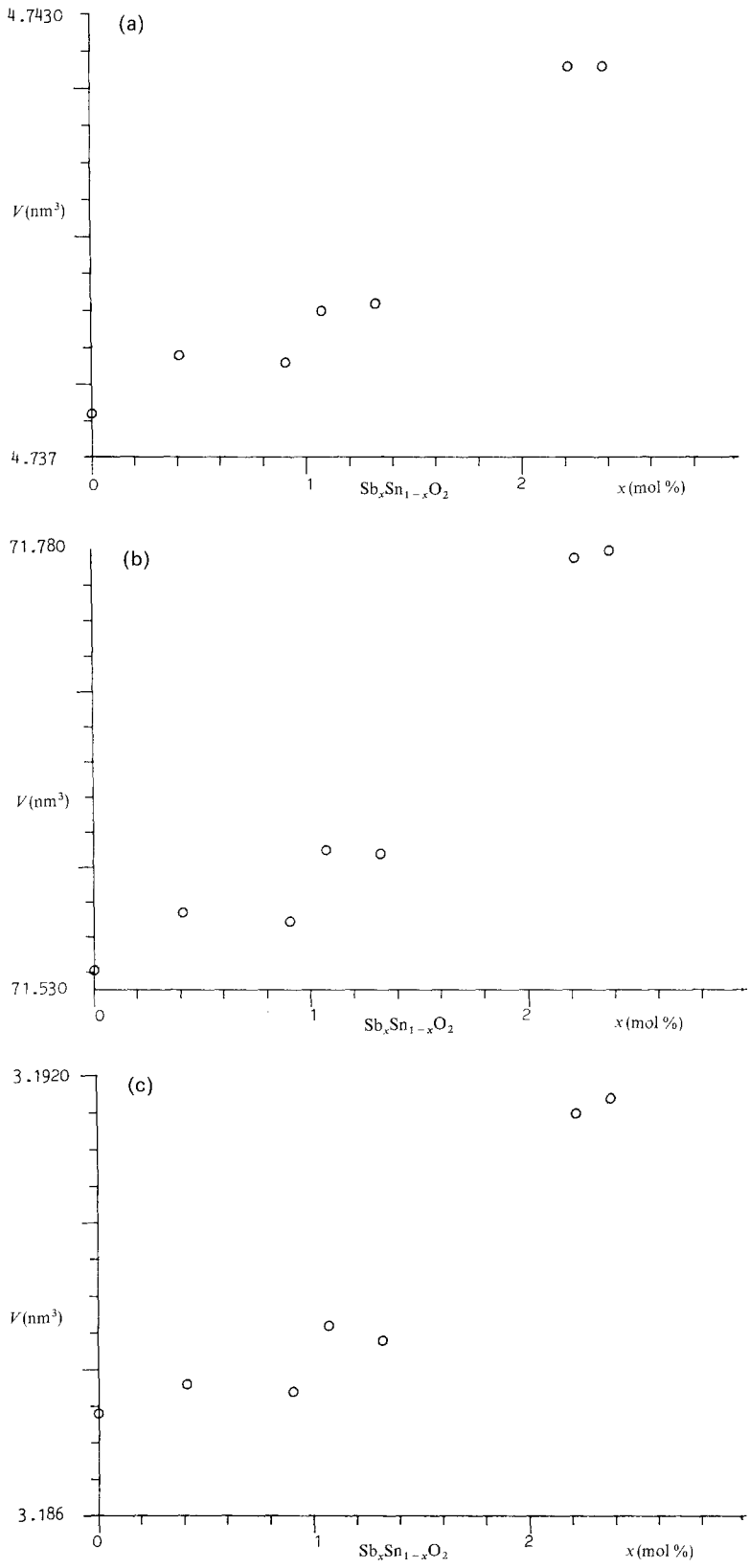


*Figure 2* Unit cell parameters as a function of concentration of dopant atoms (Sb) in $SnO_2$/Sb powders. (a) crystallographic *a*-axis, (b) crystallographic *c*-axis, (c) unit cell volume.

are the transmittance in the visible and near infrared range, and the infrared reflectance [11, 12]. It is very difficult to measure quantitatively the transmission of powdered samples in the visible and near infrared region. Owing to the high refractive index of $SnO_2$ powder ($n > 2$), elementary particles of the powder must be of the order of 0.3 to 0.4 μm in order to compensate for the effects of Mie and Rayleigh type scattering. For transmission measurements the powder was mixed with a non-absorbing vehicle (nujol), thus the correlation between the optical thickness of the nujol film and the transmission parameters was lost or was at least inaccurate. Therefore, only qualitative transmission spectra of powders containing different amounts of dopant atoms are given in Fig. 3.

It is apparent that the transmission of the samples decreases with increasing content of antimony dopant atoms. Nevertheless, the last two spectra, which correspond to samples with $x = 2.22$ and 2.38 mol %, respectively (see also Table I), have approximately equal transmission spectra. The minimum of transmission, marked with arrows in Fig. 3, shifts to shorter

TABLE I Influence of antimony content on $SnO_2$ powder properties

| Sample | Conc. $Sb^{3+}$ (mol %) | ρ (Ω cm) | $\omega_{pl,exp}$ ($cm^{-1}$) | $\omega_{pl,calc}$ ($cm^{-1}$) | $\gamma_{pl,calc}$ (cm) |
|---|---|---|---|---|---|
| 1 | 0 | 2736 | – | – | – |
| 2 | 0.41 | 13.50 | 1600 | 1070 | 1350 |
| 3 | 0.90 | 16.9 | 2200 | 1500 | 1500 |
| 4 | 1.07 | 10.24 | 2700 | 2900 | 2400 |
| 5 | 1.32 | 2 | 3000 | 2800 | 2064 |
| 6 | 2.22 | 4.5 | 3300 | 3200 | 2300 |
| 7 | 2.38 | 10.0 | 3600 | 3500 | 2700 |

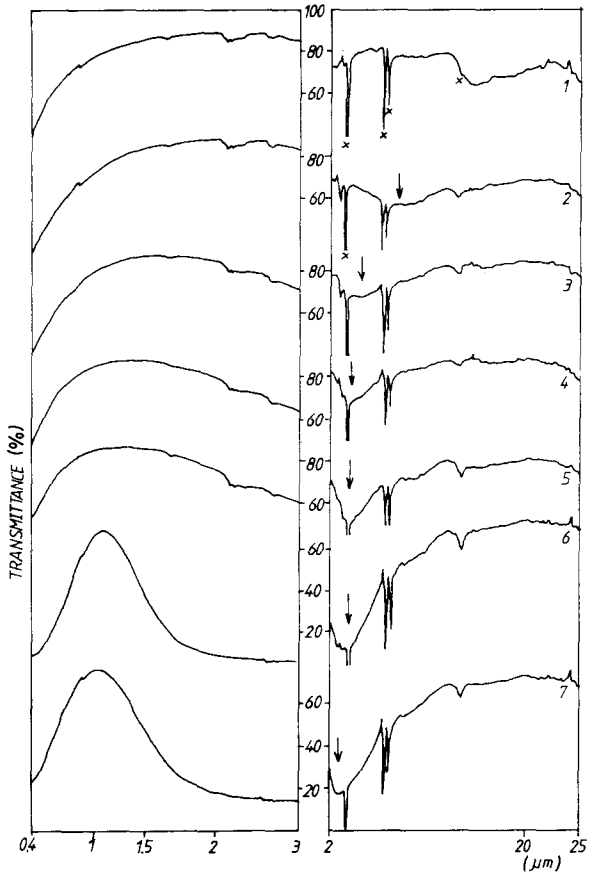


*Figure 3* Transmission spectra of $SnO_2$/Sb powders at various contents of antimony atoms. Arrows indicate transmittance minimum which corresponds to the function infrared transmittance. Dopant concentrations correspond to samples listed in Table I (x - nujol band).

wavelengths on further increasing the dopant concentration. Nevertheless, a more detailed determination of the vibrational bands of $SnO_2$ powder and the corresponding plasma oscillations appearing in the absorption spectra of the doped powders was impossible to obtain. The transmission spectra (Fig. 3) were determined only qualitatively, thus preventing calculation of exact infrared transmittance values [11].

The infrared reflection spectra (Fig. 4) indicate that the onset of the broad reflection band due to free carrier oscillations starts approximately at the same wavenumber at which the minimum in transmission spectra of nujol mulls appears (Fig. 3) for those samples containing the same amount of dopants. The intensity of the reflection maximum is increased with $x$ and at the same time is shifted to higher wavenumbers, but the part of the reflectivity curve which is close to the phonon bands (1000 to 700 $cm^{-1}$) shows some kind of saturation with $x$.

A correlation of reflectivity in the middle of the infrared range ( $\sim$ 1800 $cm^{-1}$) with dopant concentration was expected according to the results obtained on thin films [12], because reflectivity is related to the resistivity of doped $SnO_2$/Sb thin films. Our four-point sheet resistance measurements indicate that the highest conductivity values were already reached for samples with $x = 1.32$ mol % (Table I and Fig. 4, sample 5), which means that resistivity measurements do not follow exactly increase of dopant concentration. This phenomenon has been already observed for thin films and correlated with mobility of free carriers due to the formation of crystallites of various sizes [3].

Evolution of the infrared reflectivity spectra as a function of dopant concentration reveals that the phonon bands [13] which correspond to the SnO stretching at 682 and 620 $cm^{-1}$, which are well resolved for $x = 0$ (Fig. 4), become less distinct with increasing $x$. Nevertheless, the reflection minimum at 758 $cm^{-1}$ remains visible, but loses its sharpness. Additionally, similar but not so pronounced inversion of reflectivity is observed for the second minimum starting to appear at 1084 $cm^{-1}$ (sample 3, Fig. 4).

Direct observation of the reflectivity spectra does not make possible a detailed description of the phonon modes of doped $SnO_2$ crystals. Characteristic broadening of the phonon bands due to the presence of a strong plasma reflectivity band hinders detection

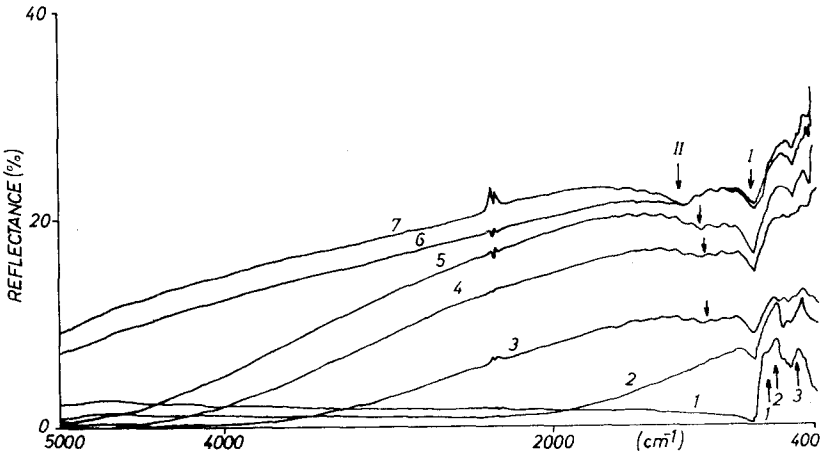


*Figure 4* Infrared reflection spectra of $SnO_2$/Sb powders. Arrows indicate phonon modes of $SnO_2$ powder: (1) 682 $cm^{-1}$, (2) 620 $cm^{-1}$, (3) 500 $cm^{-1}$. I first inversion band, II second inversion band (see text).

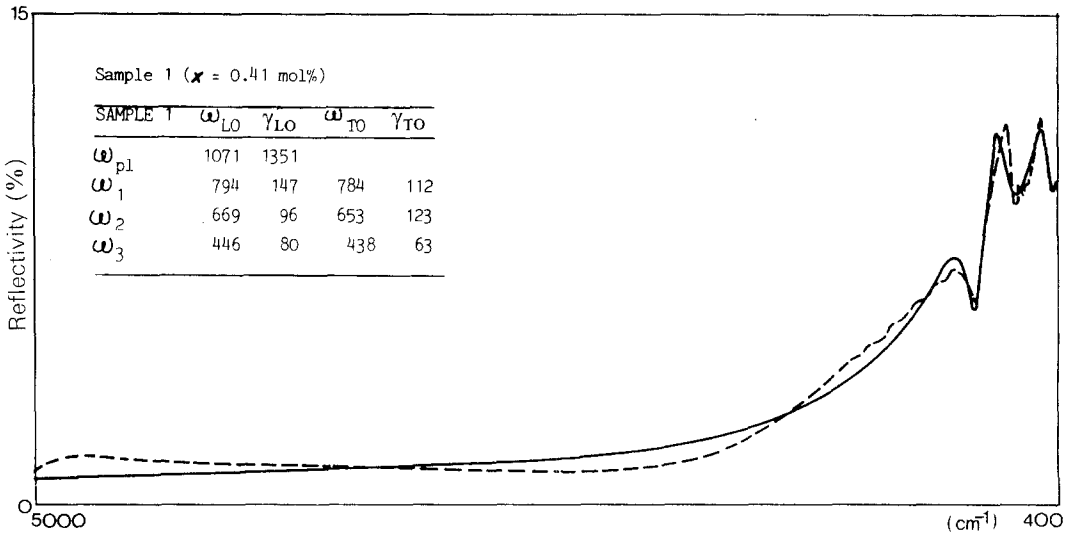


*Figure 5* Example of fitting procedure achieved for $SnO_2$/Sb ($x$ = 0.41 mol %).

of the frequency shifts and damping of the phonon modes. Model calculations based on an extended Kurosawa–Drude dispersion relation [14], which is suitable for treatment of monocrystalline systems have been also applied for $SnO_2$/Sb powder.

The dielectric function, $\varepsilon(\omega)$, was expressed by the formula

$$\varepsilon(\omega) = \varepsilon_\infty \left[ \prod_{j_{pl}} \frac{\omega_{LO}^2 - \omega^2 - i\gamma_{LO}}{\omega_{TO}^2 - \omega^2 - i\gamma_{TO}} - \frac{\omega_{pl}^2 - i(\gamma_{pl} - \gamma_0)\omega}{\omega(\omega + i\gamma_0)} \right]$$

where $\omega_{LO}$, $\omega_{TO}$, $\gamma_{LO}$, $\gamma_{TO}$ are oscillator parameters, $\omega_{pl}$ and $\gamma_{pl}$ are plasma frequency and damping, $\varepsilon_\infty$ is the dielectric constant at infinite ($\sim 4000\,cm^{-1}$) frequency, and the summation is carried out over all the observed phonon modes. The function is fitted to the reflectivity spectra (Fig. 4) according to the formula

$$R = \left( \frac{\varepsilon^{1/2} - 1}{\varepsilon^{1/2} + 1} \right)^2$$

from which the parameters listed in Table I were obtained.

One of the fitted reflectivity spectra is reproduced in Fig. 5.

We are aware of approximations which were used in our calculations. For example, the limited spectral range (4000–400 $cm^{-1}$) decreases the reliability of the calculated parameters. Nevertheless, the greatest source of error is the fact that the effects of polycrystallinity of the samples have not been considered in our calculations. For the polycrystalline samples with randomly oriented single crystals, phonon modes having different symmetries contribute in various extents to the reflectivity of the powder. The intensities of A and E phonon modes of a tetragonal $SnO_2$ monocrystal appearing in $\|c$ and $\|a$ spectra should be weighted in different ways in the reflectivity spectra in order to simulate the different participations of the randomly oriented single crystals in the powder. Moreover, the influence of the surface roughness of the powder pellets on the measured reflectivity has not been taken into account during our fitting procedure. For the above reasons, the results of the model calculations could be taken only as an indication of a blue shift (Table I) of plasma oscillations as a function of $x$, while detailed description of phonon mode shifts and their damping do not describe the phonon–plasmon interactions properly.

## 4. Conclusion

Our attempts to make highly doped $SnO_2$ powder with antimony atoms in which doping should be greater than that known for the films ($x \sim 2$ to 3 mol %) was not successful, because the highest concentrations of antimony which were achieved in our experiments did not exceed 2.38 mol% despite the very high initial concentration of $SbCl_3$ ($\simeq$ 50 mol %). The main reason was the insufficient solubility of $SbCl_3$ in the rutile phase [15].

Until cell distortion due to the dopant atoms did not exceed that reported previously by others [9], although increases of the $a$ and $c$ crystallographic axes were observed. Linearity was not achieved and might be due to the insufficient precision of analytical procedures used in our experiments.

Sheet resistance measurements revealed that for concentrations of antimony atoms higher than $x$ = 1.32 mol %, increased resistivity values appeared. Similar dependences of resistivity upon dopant concentration have been reported for thin films [12] and also for powders [5], although the minima have been achieved at higher dopant concentrations, 3 mol % and 10 wt %, respectively, [12].

Optical properties do not fully support our sheet resistance measurements. Visible transmission spectra reveal that the transparency of the powdered samples is gradually decreased with increasing $x$. Near and infrared transmission spectra support this behaviour, indicating additionally that the plasma oscillations are gradually shifted from the infrared (200 $cm^{-1}$) to the near infrared (5000 $cm^{-1}$) spectral range.

The existence of a one-to-one correspondence between the reflectivity band attributed to the plasma

oscillations and the concentration of dopant atoms was found. The evolution of the intensity of the corresponding reflectivity band is not symmetric, i.e. the peak intensity of this band is shifted from smaller to higher wavenumbers. That part of the reflectivity band which is close to the phonon modes is damped in the greatest extent and does not show an increase in intensity, while the part further away increases with dopant concentration.

At higher concentrations ($x > 1.0$ mol %), a peak in the reflectivity curve centred at $\sim 1200\,cm^{-1}$ was assigned as due to electronic absorption [10]. We found no additional experimental fact which could support this assignment. On the other hand, this band might be a spurious band which becomes apparent due to the presence of a negative reflectance peak appearing at $1084\,cm^{-1}$ which shifts up to $1186\,cm^{-1}$ with increasing dopant concentration.

Similar negative peaks are known, from molecular transmission and reflectance spectra, as Evans' bands [16] and appear due to the interactions between a weak phonon mode and closely spaced phonon levels. Recently, negative reflectance peaks have also been found in the reflectance spectra of some complex oxides exhibiting superconductivity [17]. In the latter case, the negative reflectance peaks correspond to the coupled modes between plasma oscillations and the phonon mode. Their intensities depend upon the strength of the electron–phonon interactions and is weak in the case of weak interactions.

Two negative reflectance peaks have been found in our spectra of doped $SnO_2$/Sb powders (Fig. 5). The first one (I) at $758\,cm^{-1}$ appears to be due to the vicinity of fundamental phonon modes in the region below $600\,cm^{-1}$. The second one (II) appears in the range 1084 to $1186\,cm^{-1}$and could not be directly connected with the corresponding phonon fundamental mode. Nevertheless, we have found weak features in transmission spectra at $1082\,cm^{-1}$ which indicate the existence of overtone or combinational modes in this spectral region. Nevertheless, the shape, appearance and shift with doping of the negative reflectance peak strongly support its coupled plasmon–phonon character.

## Acknowledgements

This work was supported by the Research Council of Slovenia. The analytical data were obtained by Mrs H. Vučković, whose assistance is gratefully acknowledged.

## References

1. T. ARAI, *J. Phys. Soc. Jpn* **15** (1960) 916.
2. C. M. LAMPERT, *Solar Wind Technol.* **4** (1987) 347.
3. Van der LEIJ, Thesis, Delft (1979).
4. Z. CRNJAK OREL, M. KLANJŠEK, S. KOCIJANČIČ and B. OREL, *Vestn. Slov. Kem. Drus.* **30** (1983) 169.
5. M. YOSHIZUMI and K. WAKABAYASHI, in 17th National SAMPE Technical Conference, 22–24 October, 1985.
6. M. YOSHIZUMI and K. NAKABAYASHI, *Plastics Engng* March (1987) 61.
7. K. UEMATSU, N. MIZUTANI and M. KATO, *J. Mater. Sci.* **22** (1987) 915.
8. M. K. PARIA and H. S. MAITI, *ibid.* **17** (1982) 3275.
9. T. KIKUCHI and M. UMEHARA, *J. Mater. Sci. Lett.* **4** (1985) 1051.
10. C. A. VINCENT and D. G. C. WESTON, *J. Electrochem. Soc. Solid State Sci. Technol.* **119** (1972) 519.
11. T. KARLSON, A. ROOS and C. G. RIBBING, *J. Sol. Energy Mater.* **11** (1985) 469.
12. E. SHANTI, V. DUTTA, A. BANERJEE and K. L. CHOPRA, *J. Appl. Phys.* **51** (1980) 6243.
13. R. SUNMITT, *ibid.* **39** (1968) 3762.
14. F. GERVAIS and Y. F. BAUMARD, *Solid State Commun.* **21** (1977) 861.
15. R. G. EDGEL, W. R. FLAVELL and P. TAVENER, *J. Solid State Commun.* **51** (1984) 345.
16. J. C. EVANS, *Spectrochim. Acta* **17** (1961) 129.
17. R. SUDHARSANAN, S. PERKOVITZ, B. LON, B. R. CALDWELL and G. L. CARR, in "High Temperature Superconducting Materials", edited by W. E. Hatfield and T. H. Miller (Marcel Dekker, 1981) pp. 283–8.

*Received 28 April*
*and accepted 24 August 1989*